Experimental Study of Robust Output-Based Continuous Sliding-Modes Controllers for Van der Pol Oscillator

Ahmed, H & Ríos, H

Original citation & hyperlink:
Ahmed, H & Ríos, H 2018, 'Experimental Study of Robust Output-Based Continuous Sliding-Modes Controllers for Van der Pol Oscillator' *IET Control Theory Applications*, vol (in press), pp. (in press)
https://dx.doi.org/10.1049/iet-cta.2017.1142

DOI 10.1049/iet-cta.2017.1142
ISSN 1751-8644
ESSN 1751-8652

Publisher: Institute of Engineering and Technology

Experimental Study of Robust Output-Based Continuous Sliding-Modes Controllers for Van der Pol Oscillator

Hafiz Ahmed, Héctor Ríos

Abstract

Robust output tracking control of Van der Pol oscillator is an important practical problem from an application point of view. Output feedback based robust tracking control strategies are proposed in this work for that purpose. First, a High-Order Sliding-Mode Observer (HOSM-O) is used to estimate the oscillator states from the measurable output and to identify some type of disturbances. Then, five different Continuous Sliding-Modes Controllers (Continuous-SMCs) are provided to robustly track a desired time-varying trajectory, exponentially or in a finite time, for the Van der Pol oscillator despite the presence of external disturbances. The closed-loop stability for each Continuous-SMC is given based on input-to-state stability (ISS) properties. Finally, experimental validations are also provided to show the feasibility of the proposed controllers in real-time.

I. Introduction

Most of real practical systems are nonlinear and of second order *e.g.*, inverted pendulum [1], DC servomotor [2], oscillator [3], robotic manipulator [4]. As such, the robust control of second order nonlinear systems attracted a lot of attention from the control community. To test the developed algorithms, several benchmark models are considered standard in the literature. One such model is Van der Pol oscillator. This model has been applied in several practical fields as well *e.g.*, biomedical engineering [5], power system [6], environmental monitoring [7], robotics [8]. As a result, robust tracking control of Van der Pol oscillator has important practical significance.

Various works have already been reported in the literature for the control of nonlinear systems like Van der Pol oscillator. In [3], a robust controller with integral filter is applied to Van der Pol oscillator. The controller of [3] can reject matched perturbations but the number of control parameters to tune is high. Moreover, the controller assumes full state measurement which limits the implementation. Experimental validations are also not provided. A first order sliding-mode controller with low pass filters has been proposed in [9]. To implement this controller, additional information of the system is required to tune the low-pass filters. Moreover, it assumes full state feedback as well. Some other results are also available in the literature using Neural Networks [10], [11]. However, the resulting controllers provide only the boundedness of the output tracking error. So, there exists scope to provide robust tracking control strategies for Van der Pol oscillator using output feedback only. This is the objective of this paper.

Out of various choices (e.g. neural network [12], adaptive control [13], Sliding-Mode Control (SMC) [14], [15], [16], [17], [18], [3], [19], [20], [21], [22], [23]) for the robust tracking control of Van der Pol oscillator, in this work SMC will be considered. SMC is one of the most promising robust control techniques. SMC has several very appealing properties like robustness with respect to parametric uncertainties and disturbances, finite-time convergence *etc*. However, the control signal is discontinuous. This discontinuity introduces high-frequency switching or "chattering" in practical implementation. Except some application areas like power electronics [24], discontinuous control signal is not desirable in many applications. To overcome the effect of chattering, several solutions have been proposed in the literature *e.g.*, [21], [22], [19], [25]. One of the most popular methods is the super-twisting algorithm (STA) which generates continuous control signal. One can apply the STA to alleviate the chattering in systems with relative degree two. Most of the practical second order nonlinear systems satisfy this condition.

In this work, using STA and its various extensions, the objective is to provide several *Continuous*-SMCs for robust tracking control of Van der Pol oscillator. These controllers can provide continuous control signals and also reject matched perturbations. In this work, it is assumed that only the output signal is available for measurement unlike [3], [9]. So, HOSM-O [20] will be used to estimate the states and perturbations of the Van der Pol oscillator. The closed-loop stability for each *Continuous*-SMC is given based on ISS properties. Moreover, experimental validation is also another objective. It is to be noted here that although this article consider Van der Pol oscillator only, the proposed controllers can be used for any other systems that share similar model structure e.g., DC servomotor [15], robotic manipulator [4]. The main idea of this work can be summarized as follows: design of a HOSM-O to estimate the states and perturbation of Van der Pol oscillator followed by the development of several *Continuous*-SMCs for robust output tracking.

School of Mechanical, Aerospace \& Automotive Engineering, Coventry University, Coventry CV1 5FB, United Kingdom. E-mail: ac7126@coventry.ac.uk
CONACYT - TECNM/Instituto Tecnólogico de La Laguna, División de Estudios de Posgrado e Investigación, Blvd. Revolución y Cuauhtémoc S/N, C.P. 27000, Torreón, Coahuila, México

The contributions of this work over the existing literature [26], [20], [19], [22], [21] can be summarized as below: first of all, unlike the existing literature, this article focus only on Van der Pol oscillator but the control strategy can be applied to any system with similar model structure. As a result, the development of several observer based *Continuous*-SMCs for Van der Pol oscillator is the first contribution. Moreover, the second novelty is the closed-loop stability analysis for each *Continuous*-SMC based on ISS properties. Finally, unlike the existing literature, experimental validations using rapid prototyping tool are provided.

The rest of the article is organized as follows: Section II gives the formal problem statement while some preliminaries are given in Section III. HOSM observer based robust tracking controllers design can be found in Section IV. Results and discussions are given in Section V. Section VI concludes this article.

II. Problem Statement

The model of the Van der Pol oscillator with external disturbances can be written as

$$\dot{x}_1 = x_2, \tag{1a}$$
$$\dot{x}_2 = -x_1 + \varepsilon x_2(1 - x_1^2) + w\,(t) + u, \tag{1b}$$
$$y = x_1, \tag{1c}$$

where $\varepsilon > 0$ is the model parameter, $x = (x_1, x_2)^T \in \mathbb{R}^2$, $u \in \mathbb{R}$, $y \in \mathbb{R}$, and $w \in \mathbb{R}$ are the state, the control input, the measurable output, and the unknown but bounded and Lipschitz external disturbance, *i.e.* $|\dot{w}(t)| \leq w^+$, for almost all $t \geq 0$ and with w^+ a known positive constant, respectively.

The control objective is to ensure that the system output y tracks a desired time-varying trajectory $y_d(t) \in \mathcal{C}^\infty$ in a finite time despite the presence of external disturbance $w(t)$. To quantify the tracking objective, a trajectory tracking error is defined as

$$y_e(t) = y(t) - y_d(t). \tag{2}$$

Thus, the control objective is equivalent to synthesizing a robust control input u, based on the state estimation from the measurement y, given by a robust observer, such that $y_e(t)$ converges to zero in a finite time.

III. Preliminaries

A. Notation

Throughout the paper the following notations are used:

- $\mathbb{R}_+ = \{x \in \mathbb{R} \colon x \geq 0\}$, where $\mathbb{R}$ is the set of all real numbers.
- Denote a sequence of integers $1, ..., n$ as $\overline{1, n}$.
- $|\cdot|$ denotes the absolute value in $\mathbb{R}$, $||\cdot||$ denotes the Euclidean norm on $\mathbb{R}^n$.
- For a (Lebesgue) measurable function $d : \mathbb{R}_+ \to \mathbb{R}^m$ define the norm $||d||_{[t_0,t_1)} = \text{ess sup}_{t\in[t_0,t_1)}||d\,(t)\,||$, then $||d||_\infty = ||d||_{[0,+\infty)}$ and the set of $d(t)$ with the property $||d||_\infty < +\infty$ is denoted as $\mathcal{L}_\infty$ (the set of essentially bounded measurable functions); and $\mathcal{L}_D = \{d \in \mathcal{L}_\infty : ||d||_\infty \leq D\}$ for any $D > 0$.
- A continuous function $\alpha : \mathbb{R}_+ \to \mathbb{R}_+$ belongs to class $\mathcal{K}$ if it is strictly increasing and $\alpha(0) = 0$; it belongs to class $\mathcal{K}_\infty$ if it is also unbounded. A continuous function $\beta : \mathbb{R}_+ \times \mathbb{R}_+ \to \mathbb{R}_+$ belongs to class $\mathcal{KL}$ if for each fixed s, $\beta(\cdot, s) \in \mathcal{K}$, and $\beta(r, \cdot)$ is strictly decreasing to zero for any fixed $r \in \mathbb{R}_+$while β belongs to class $\mathcal{KL}_T$ if for each fixed s, $\beta(\cdot, s) \in \mathcal{K}$, and for each fixed r there exists $0 < T(r) < \infty$ such that $\beta(r, s)$ is decreasing to zero with respect to $s < T(r)$, and $\beta(r, s) = 0$ for all $s \geq T(r)$.

B. Stability of Nonlinear Systems

This section gives the notion of different types of stability of nonlinear systems. These notions will be helpful to understand the type of convergence of the proposed differentiator based control strategy given in Section IV.

Consider the following nonlinear system

$$\dot{x}\,(t) = f\,(x\,(t)\,, d\,(t))\,, t \geq 0, \tag{3}$$

where $x\,(t) \in \mathbb{R}^n$ is the state, $d\,(t) \in \mathbb{R}^m$ is the external input such that $d \in \mathcal{L}_\infty$, $f \colon \mathbb{R}^{n+m} \to \mathbb{R}^n$ ensures forward existence of the system solutions at least locally, $f\,(0, 0) = 0$. For an initial condition $x_0 \in \mathbb{R}^n$ and input $d \in \mathcal{L}_\infty$, define the corresponding solution by $\varphi(t, x_0, d)$, for any $t \geq 0$ for which the solution exists. Let Ω be an open neighborhood of the origin in $\mathbb{R}^n$ and $D > 0$.

Definition 1. *At the steady state $x = 0$, the system (3), for $d \in \mathcal{L}_D$, is said to be*

a) Uniformly Lyapunov Stable (US) *if for any $x_0 \in \Omega$ and $d \in \mathcal{L}_D$ the solution $\varphi(t, x_0, d)$ is defined for all $t \geq 0$, and for any $\varepsilon > 0$ there is $\delta(\varepsilon) > 0$ such that for any $x_0 \in \Omega$, if $||x_0|| < \delta(\varepsilon)$ then $||\varphi(t, x_0, d)|| < \varepsilon$ for all $t \geq 0$;*

b) Uniformly Exponentially Stable (UES) *if it is uniformly Lyapunov stable in Ω and exponentially converging from Ω, i.e. for any $x_0 \in \Omega$ there exist κ, $\gamma > 0$ such that $||\varphi(t, x_0, d)|| < \kappa ||x_0|| e^{-\gamma t}$ for all $t \geq 0$;*

c) Uniformly Finite-Time Stable (UFTS) *if it is uniformly Lyapunov stable in Ω and uniformly finite-time converging from Ω, i.e. for any $x_0 \in \Omega$ and all $d \in \mathcal{L}_D$ there exists $0 \leq T \leq +\infty$ such that $\varphi(t, x_0, d) = 0$ for all $t \geq T$. The function $T_0(x_0) = inf\{T \geq 0 \colon \varphi(t, x_0, d) = 0 \, \forall t \geq T, \forall d \in \mathcal{L}_D\}$ is called* the uniform settling time *of the system (3).*

If $\Omega = \mathbb{R}^n$, then the corresponding properties are called global uniform Lyapunov/exponential/finite-time stability of (3) for $d \in \mathcal{L}_D$ at $x = 0$. For details, please consult [27] and the references therein.

C. Homogeneity

For any $r_i > 0$, $i = \overline{1, n}$, and $\lambda > 0$, define the dilation matrix $\Lambda_r(\lambda) = \text{diag}\{\lambda^{r_i}\}_{i=1}^n$, the vector of weights $r = (r_1, \ldots, r_n)^T$, and the homogeneous norm, defined for any $x \in \mathbb{R}^n$, as follows

$$||x||_r = \left(\sum_{i=1}^{n} ||x_i||^{\frac{\rho}{r_i}} \right)^{\frac{1}{\rho}}, \; \rho = \prod_{i=1}^{n} r_i.$$

For all $x \in \mathbb{R}^n$, its Euclidean norm $||x||$ is related with the homogeneous one [28]:

$$\underline{\alpha}_r(||x||_r) \leq ||x|| \leq \overline{\alpha}_r(||x||_r), \tag{4}$$

for some $\underline{\alpha}_r, \overline{\alpha}_r \in \mathcal{K}_\infty$. Due to this "equivalence", stability analysis with respect to the norm $||x||$ may be substituted with analysis for the norm $||x||_r$. The homogeneous norm has an important property that is $||\Lambda_r(\lambda)x||_r = \lambda ||x||_r$ for all $x \in \mathbb{R}^n$. Define $\mathbb{S}_r = \{x \in \mathbb{R}^n : ||x||_r = 1\}$.

Definition 2. [29] *The function $g : \mathbb{R}^n \to \mathbb{R}$ is called r-homogeneous ($r_i > 0$, $i = \overline{1, n}$), if for any $x \in \mathbb{R}^n$ the relation $g(\Lambda_r(\lambda)x) = \lambda^q g(x)$, holds for some $q \in \mathbb{R}$ and all $\lambda > 0$. The function $f : \mathbb{R}^n \to \mathbb{R}^n$ is called r-homogeneous ($r_i > 0$, $i = \overline{1, n}$), if for any $x \in \mathbb{R}^n$ the relation $f(\Lambda_r(\lambda)x) = \lambda^q \Lambda_r(\lambda) f(x)$, holds for some $q \geq -\min_{1 \leq i \leq n} r_i$ and all $\lambda > 0$. In both cases, the constant q is called the degree of homogeneity.*

Homogeneous systems possess certain robustness with respect to external disturbances. Consider a system described by the following differential inclusion

$$\dot{x}(t) \in F(x(t), d(t)), \; t \geq 0, \tag{5}$$

where x and d have the same meaning as in *(3)*, and $F : \mathbb{R}^{n+m} \rightrightarrows \mathbb{R}^n$ is a set-valued map. Similarly to system 3, for an initial condition $x_0 \in \mathbb{R}^n$ and input $d \in \mathcal{L}_\infty$, define the corresponding solution by $\varphi(t, x_0, d)$, for any $t \geq 0$ and denote by $\mathbb{S}(x_0)$ as the set of solutions $\varphi(t, x_0, d)$ corresponding to the common initial condition x_0.

Definition 3. [30] *System (5) is said to be finite-time input-to-state stable (FT-ISS) if for all $x_0 \in \mathbb{R}^n$ and $d \in \mathcal{L}_D$ the estimate*

$$||\varphi(t, x_0, d)|| \leq \beta(||x_0||, t) + \gamma(||d||_\infty),$$

holds for all $t \geq 0$ and $\varphi(t, x_0, d) \in \mathbb{S}(x_0)$ for some $\beta \in \mathcal{KL}_T$ and $\gamma \in \mathcal{K}$.

Definition 4. [30] *System (5) is said to be finite-time integral input-to-state stable (FT-iISS) if for all $x_0 \in \mathbb{R}^n$ and $d \in \mathcal{L}_D$ the estimate*

$$\alpha(||\varphi(t, x_0, d)||) \leq \beta(||x_0||, t) + \int_0^t \gamma(||d(\tau)||_\infty) d\tau,$$

holds for all $t \geq 0$ and $\varphi(t, x_0, d) \in \mathbb{S}(x_0)$ for some $\alpha \in \mathcal{K}_\infty$, $\beta \in \mathcal{KL}_T$ and $\gamma \in \mathcal{K}$.

For a system represented by the differential equation (3), the classic definitions of ISS and iISS can be obtained if it is assumed that $\beta \in \mathcal{KL}$ (see, for instance [31]).

Let us denote an extended discontinuous function $\tilde{F}(x, d) = (F^T(x, d), 0_m)^T$.

Theorem 1. [30] *Let $\tilde{F}$ be homogeneous with weights $r = (r_1, \ldots, r_n) > 0$ and $\tilde{r} = (\tilde{r}_1, \ldots, \tilde{r}_m) \geq 0$ with a degree $q \geq -\min_{1 \leq i \leq n} r_i$, i.e. $F(\Lambda_r x, \Lambda_{\tilde{r}} d) = \lambda^q \Lambda_r F(x, d)$. Assume that the system (5) is globally asymptotically stable for $d = 0$. Let*

$$||F(z, d) - F(z, 0)|| \leq \sigma(||d||), \; \forall z \in \mathbb{S}_r,$$

$$\sigma(s) = \begin{cases} c s^{\rho_{\min}}, & if \; s \leq 1, \\ c s^{\rho_{\max}}, & if \; s > 1, \end{cases}$$

for some $c > 0$ and $\rho_{\max} \geq \rho_{\min} > 0$. Then, the system (5) is:

a) ISS *if $\tilde{r}_{\min} > 0$, where $\tilde{r}_{\min} = \min_{1\leq j\leq m} \tilde{r}_j$;*

b) iISS *if $\tilde{r}_{\max}\rho_{\min} - \mu \leq q \leq \tilde{r}_{\min} = 0$, where $\tilde{r}_{\max} = \max_{1\leq j\leq m} \tilde{r}_j$ and some $\mu > 0$.*

If the homogeneity degree $q < 0$, then the system (5) is FT-ISS *or* FT- iISS*, respectively.*

IV. Robust Tracking Controllers Design

In the following the design of the proposed control strategies to tracking the Van der Pol oscillator output is addressed. The proposed robust tracking is composed by a HOSM-O and the possibility to use five different *Continuous*-SMCs. Firstly, the design of the HOSM-O is presented.

A. Finite-Time Sliding-Mode Observer

Consider the following HOSM-O

$$\dot{\hat{x}}_1 = \hat{x}_2 + \hat{k}_1 \lceil \hat{e}_1 \rfloor^{\frac{2}{3}}, \tag{6a}$$

$$\dot{\hat{x}}_2 = -x_1 + \varepsilon \hat{x}_2(1 - x_1^2) + u + \hat{x}_3 + \hat{k}_2 \lceil \hat{e}_1 \rfloor^{\frac{1}{3}}, \tag{6b}$$

$$\dot{\hat{x}}_3 = \hat{k}_3 \lceil \hat{e}_1 \rfloor^{0}, \tag{6c}$$

where $\hat{e}_1 := x_1 - \hat{x}_1$ is the output error, the function $\lceil \cdot \rfloor^{\gamma} := |\cdot|^{\gamma}\text{sign}(\cdot)$, for any $\gamma \in \mathbb{R}_{\geq 0}$; and some design parameters $\hat{k}_i$, $i = \overline{1,3}$. Define the state estimation error as $\hat{e} := (\hat{e}_1, \hat{e}_2)^T \in \mathbb{R}^2$, where $\hat{e}_2 := x_2 - \hat{x}_2$. Let us introduce the following assumption.

Assumption 1. *Suppose that there exists $\xi > 0$ such that the following inequality is satisfied:*

$$\left\| \frac{d}{dt} \left(f(x_1, \hat{e}_2) + w \right) \right\|_{\infty} \leq \xi,$$

where $f(x_1, \hat{e}_2) := \varepsilon \hat{e}_2(1 - x_1^2)$.

Note that, due to the boundedness properties of the Van der Pol oscillator and the fact that the disturbance w is Lipschitz, Assumption 1 always holds. Then, the following theorem describes the convergence properties of the HOSM-O.

Theorem 2. *Let the observer (6) be applied to system (1) and Assumption 1 be satisfied. If the observer parameters are chosen as follows:*

$$\hat{k}_1 = 3\xi^{\frac{1}{3}}, \ \hat{k}_2 = 1.5\xi^{\frac{1}{2}}, \ \hat{k}_3 = 1.1\xi,$$

then the state estimation error $\hat{e} = 0$ is UFTS.

Proof: The error dynamics between system (1) and the HOSM-O (6) is given as follows:

$$\dot{\hat{e}}_1 = \hat{e}_2 - \hat{k}_1 \lceil \hat{e}_1 \rfloor^{\frac{2}{3}}, \tag{7a}$$

$$\dot{\hat{e}}_2 = \varepsilon \hat{e}_2(1 - x_1^2) + w - \hat{x}_3 - \hat{k}_2 \lceil \hat{e}_1 \rfloor^{\frac{1}{3}}, \tag{7b}$$

$$\dot{\hat{x}}_3 = \hat{k}_3 \lceil \hat{e}_1 \rfloor^{0}. \tag{7c}$$

Define $\hat{e}_3 := \varepsilon \hat{e}_2(1 - x_1^2) + w - \hat{x}_3$, then (7) may be written as

$$\dot{\hat{e}}_1 = \hat{e}_2 - \hat{k}_1 \lceil \hat{e}_1 \rfloor^{\frac{2}{3}}, \tag{8a}$$

$$\dot{\hat{e}}_2 = \hat{e}_3 - \hat{k}_2 \lceil \hat{e}_1 \rfloor^{\frac{1}{3}}, \tag{8b}$$

$$\dot{\hat{e}}_3 = -\hat{k}_3 \lceil \hat{e}_1 \rfloor^{0} + \dot{f} + \dot{w}, \tag{8c}$$

It is clear that the previous dynamics is the same that the second-order sliding-mode differentiator given by [20]. The error dynamics (8) is homogeneous of degree $q = -1$ and weights $r = (3, 2, 1)$. Hence, based on homogeneity and Lyapunov theory, one can show that the error dynamics (8) is finite-time stable.

In this sense, in [32] , it has been shown that System (8) admits the following strong, proper, smooth and homogeneous of degree $q = 5$ with weights $r = (3, 2, 1)$, Lyapunov function

$$V(\hat{e}) = \alpha_1 |\hat{e}_1|^{\frac{5}{3}} - \beta_1 \hat{e}_1 \hat{e}_2 + \alpha_2 |\hat{e}_2|^{\frac{5}{2}} - \beta_2 \hat{e}_2 \hat{e}_3^3 + \alpha_3 |\hat{e}_3|^5,$$

with some positive constants α_j, $j = \overline{1,3}$ and β_i, $i = 1, 2$. Moreover, considering that Assumption 1 holds, then there exist some positive constants $\hat{k}_i$, α_i, $i = \overline{1,3}$ and β_j, $j = 1, 2$ such that $\hat{e} = 0$ is *UFTS*; and hence, $\hat{x}_1(t) = x_1(t)$, $\hat{x}_2(t) = x_2(t)$ and $\hat{x}_3(t) = f(x_1(t), \hat{e}_2(t)) + w(t)$, for all $t \geq \hat{T}$.

Particularly, in [20] it has been shown that the set of gains $\hat{k}_1 = 3\xi^{\frac{1}{3}}$, $\hat{k}_2 = 1.5\xi^{\frac{1}{2}}$ and $\hat{k}_3 = 1.1\xi$ provides finite-time convergence for system (8). This concludes the proof. ∎

In the following sections five different *Continuous* Sliding-Modes Control strategies are presented in order to track a desired time-varying trajectory, exponentially or in a finite time, despite the presence of external disturbances.

B. Linear Control Design

Let us consider the following compensation-based controller

$$u = -u_{eq} + \ddot{y}_d - k_1 e_1 - k_2 \bar{e}_2, \tag{9a}$$

$$u_{eq} = -x_1 + \varepsilon \hat{x}_2 (1 - x_1^2) + \hat{x}_3, \tag{9b}$$

where $e_1 := x_1 - y_d$ and $\bar{e}_2 := \hat{x}_2 - \dot{y}_d$ are the output tracking errors while k_1 and k_2 are some positive design gains. Define the tracking error as $e := (e_1, e_2)^T \in \mathbb{R}^2$, where $e_2 := x_2 - \dot{y}_d$. Then, the following result is established.

Theorem 3. *Let the observer (6) and the controller (9) be applied to system (1) and Assumption 1 be satisfied. If the observer parameters are chosen as in Theorem 1 and the controller gains $k_1, k_2 > 0$, then the tracking error $e = 0$ is Uniformly Exponentially Stable, for all $(\dot{f} + \dot{w}) \in \mathcal{L}_\xi$.*

Proof: The tracking error dynamics is given by

$$\dot{e}_1 = e_2, \tag{10a}$$

$$\dot{e}_2 = -x_1 + \varepsilon x_2 (1 - x_1^2) + w + u - \ddot{y}_d. \tag{10b}$$

Let us substitute the controller (9) into (10). Note that $\bar{e}_2$ can be expressed as $\bar{e}_2 = e_2 - \hat{e}_2$. Thus, the closed-loop dynamics is written as:

$$\Pi_l : \begin{cases} \dot{e}_1 = e_2, \\ \dot{e}_2 = -k_1 e_1 - k_2 e_2 + k_2 \hat{e}_2 + \hat{e}_3, \end{cases} \tag{11a}$$

$$\Pi_2 : \begin{cases} \dot{\hat{e}}_1 = \hat{e}_2 - \hat{k}_1 \lceil \hat{e}_1 \rfloor^{\frac{2}{3}}, \\ \dot{\hat{e}}_2 = \hat{e}_3 - \hat{k}_2 \lceil \hat{e}_1 \rfloor^{\frac{1}{3}}, \\ \dot{\hat{e}}_3 = -\hat{k}_3 \lceil \hat{e}_1 \rfloor^0 + \dot{f} + \dot{w}. \end{cases} \tag{11b}$$

According to Theorem 2, the trajectories of the system Π_2 converge to zero in a finite time. Then, since the trajectories of the system Π_l do not grow faster than an exponential, *i.e.* they do not escape to infinity in a finite time, one can assume that $\hat{e} = 0$. Hence, the closed-loop dynamics (11) is reduced to

$$\dot{e}_1 = e_2, \tag{12a}$$

$$\dot{e}_2 = -k_1 e_1 - k_2 e_2. \tag{12b}$$

Therefore, for any $k_1, k_2 > 0$, one can show that $e = 0$ is *UES*. Thus $x_1(t) \to y_d(t)$ and $x_2(t) \to \dot{y}_d(t)$ as $t \to \infty$. The proof is concluded. ■

C. Super-Twisting Control Design

Let us consider the Super-Twisting Control (see [20] and [26]), *i.e.*

$$s = \bar{e}_2 + k_1 e_1, \tag{13a}$$

$$u = -u_{eq} + \ddot{y}_d + v - k_2 \lceil s \rfloor^{\frac{1}{2}}, \tag{13b}$$

$$u_{eq} = -x_1 + \varepsilon \hat{x}_2 (1 - x_1^2) + \hat{x}_3 + \hat{k}_2 \lceil \hat{e}_1 \rfloor^{\frac{1}{3}} + k_1 \bar{e}_2, \tag{13c}$$

$$\dot{v} = -k_3 \lceil s \rfloor^0, \tag{13d}$$

for some positive constants k_i, $i = \overline{1,3}$. The following result is stated.

Theorem 4. *Let the observer (6) and the controller (13) be applied to system (1) and Assumption 1 be satisfied. Let the observer parameters be chosen as in Theorem 2 and suppose that there exist matrices $0 < P^T = P \in \mathbb{R}^{2\times 2}$ and $Y \in \mathbb{R}^{2\times 1}$, and a positive constant $\alpha > 0$ such that the linear matrix inequality*

$$PA + A^T P - YC - C^T Y^T + \alpha I \leq 0, \tag{14}$$

$$A := \begin{pmatrix} 0 & 1 \\ 0 & 0 \end{pmatrix}, \; B := \begin{pmatrix} 0 \\ 1 \end{pmatrix}, \; C^T := \begin{pmatrix} 1 \\ 0 \end{pmatrix},$$

is feasible. Then, for $(k_2, k_3)^T = P^{-1} Y$ and any $k_1 > 0$, the tracking error $e = 0$ is Uniformly Exponentially Stable, for all $(\dot{f} + \dot{w}) \in \mathcal{L}_\xi$, and the quadratic form $V = \zeta^T P \zeta$, with $\zeta^T = \begin{pmatrix} \lceil s \rfloor^{\frac{1}{2}} & v \end{pmatrix}$, is a strong and robust Lyapunov function for system (10)*.*

Proof: Substituting (13) in the tracking error dynamics (10), one obtains

$$\dot{e}_1 = e_2, \tag{15a}$$
$$\dot{e}_2 = -k_1\bar{e}_2 - \hat{k}_2 \lceil \hat{e}_1 \rfloor^{\frac{1}{3}} + v - k_2 \lceil s \rfloor^{\frac{1}{2}} + \hat{e}_3, \tag{15b}$$
$$\dot{v} = -k_3 \lceil s \rfloor^{0}, \tag{15c}$$

and then, recalling that $\bar{e}_2 = e_2 - \hat{e}_2$ and $s = \bar{e}_2 + k_1 e_1$, the closed-loop dynamics can be given as

$$\Pi_1 : \{ \ \dot{e}_1 = s - k_1 e_1, \tag{16a}$$
$$\Pi_{st} : \begin{cases} \dot{s} = v - k_2 \lceil s \rfloor^{\frac{1}{2}} + k_1 \hat{e}_2, \\ \dot{v} = -k_3 \lceil s \rfloor^{0}, \end{cases} \tag{16b}$$
$$\Pi_2 : \begin{cases} \dot{\hat{e}}_1 = \hat{e}_2 - \hat{k}_1 \lceil \hat{e}_1 \rfloor^{\frac{2}{3}}, \\ \dot{\hat{e}}_2 = \hat{e}_3 - \hat{k}_2 \lceil \hat{e}_1 \rfloor^{\frac{1}{3}}, \\ \dot{\hat{e}}_3 = -\hat{k}_3 \lceil \hat{e}_1 \rfloor^{0} + \dot{f} + \dot{w}. \end{cases} \tag{16c}$$

Note that system (16) can be viewed as a cascade system where Π_2 is the input of Π_{st}, and in turn, Π_{st} the input of Π_1.

Once again, according to Theorem 2, the trajectories of the system Π_2 converge to zero in a finite time. Therefore, it follows that for all $|\dot{f} + \dot{w}|_\infty \leq \xi$

$$||\hat{e}(t, \hat{e}_0, \dot{f} + \dot{w})|| \leq \delta_{\hat{e}}, \ \forall t \geq 0,$$

with some $\delta_{\hat{e}} \geq 0$. On the other hand, it is clear that Π_{st} has the same structure as the Super-Twisting algorithm except for the bounded external input $\hat{e}_2$. Let us define the following set-valued map

$$\tilde{F}(s, v, \hat{e}_2) = \begin{pmatrix} F(s, v, \hat{e}_2) \\ 0 \end{pmatrix} = \begin{pmatrix} v - k_2 \lceil s \rfloor^{\frac{1}{2}} + k_1 \hat{e}_2 \\ -k_3 \lceil s \rfloor^{0} \\ 0 \end{pmatrix}.$$

Such a discontinuous function is homogeneous of degree $q = -1$ and weights $r = (2, 1)$ and $\tilde{r} = 1$. In [33], it has been shown that, for $\hat{e}_2 = 0$, the quadratic form $V = \zeta^T P \zeta$, with $\zeta^T = (\ \lceil s \rfloor^{\frac{1}{2}} \quad v\ )$ and P satisfying (14), is a strong and robust Lyapunov function for Π_{st}. Thus, $(s, v) = 0$ is *UFTS*. Moreover, it follows that

$$||F(s, v, \hat{e}_2) - F(s, v, 0)|| = k_1 ||\hat{e}_2|| \leq \sigma(||\hat{e}_2||), \ \forall s, v \in \mathbb{R},$$
$$\sigma(s) = \begin{cases} c s^{\rho_{\min}}, & if \ s \leq 1, \\ c s^{\rho_{\max}}, & if \ s > 1, \end{cases}$$

for $c \geq k_1$ and $\rho_{\max} = \rho_{\min} = 1$. Therefore, all the conditions of Theorem 1 are satisfied, and since $\tilde{r}_{\min} = 1 > 0$, system Π_{st} is *FT-ISS* with respect to the bounded input $\hat{e}_2$, *i.e.*

$$\left\| \begin{matrix} s(t, s_0, \hat{e}_2) \\ v(t, v_0, \hat{e}_2) \end{matrix} \right\| \leq \beta_{st} \left(\left\| \begin{matrix} s_0 \\ v_0 \end{matrix} \right\|, t \right) + \gamma_{\hat{e}1}(||\hat{e}_2||_\infty), \tag{17}$$

for all $t \geq 0$ and some $\beta_{st} \in \mathcal{KL}_T$ and $\gamma_{\hat{e}1} \in \mathcal{K}$. Moreover, since for system Π_2, $\hat{e} = 0$ is *UFTS*, one obtains that (17) satisfies

$$\left\| \begin{matrix} s(t, s_0, \hat{e}_2) \\ v(t, v_0, \hat{e}_2) \end{matrix} \right\| \leq \beta_{st} \left(\left\| \begin{matrix} s_0 \\ v_0 \end{matrix} \right\|, t \right) + \gamma_{\hat{e}2}(||\hat{e}_2(0)||, t),$$

for all $t \geq 0$ and some $\beta_{st}, \gamma_{\hat{e}2} \in \mathcal{KL}_T$. This implies that also $(s, v) = 0$ is *UFTS* for any $\hat{e}_2 \in \mathbb{R}$. Finally, it is easy to show that system Π_1 is *ISS* with respect to the input s, *i.e.*

$$||\ e_1(t, e_1(0), s)|| \ \leq \beta_{e1}(||e_1(0)||, t) + \gamma_{s1}(||s||_\infty), \tag{18}$$

for all $t \geq 0$ and some $\beta_{e1} \in \mathcal{KL}$ and $\gamma_{s1} \in \mathcal{K}$. Then, due to the fact that $(s, v) = 0$ is *UFTS*, (18) satisfies

$$||\ e_1(t, e_1(0), s)|| \ \leq \beta_{e1}(||e_1(0)||, t) + \gamma_{s2}(||s_0||, t),$$

for all $t \geq 0$, $\beta_{e1}(||e_1(0)||, t) = ||e_1(0)||e^{-k_1 t}$ and some $\gamma_{s2} \in \mathcal{KL}_T$. Evidently, $e_1 = 0$, and hence $\bar{e}_2 = 0$, are *UES* for any $k_1 > 0$. Thus $x_1(t) \to y_d(t)$ and $x_2(t) \to \dot{y}_d(t)$ as $t \to \infty$. This concludes the proof. ■

D. Continuous Singular Terminal Sliding-Mode Control Design

Consider now the Continuous Singular Terminal Sliding-Mode control (*Continuous*-STSMC) [19], *i.e.*

$$s = \bar{e}_2 + k_1 \lceil e_1 \rfloor^{\frac{2}{3}}, \tag{19a}$$

$$u = -u_{eq} + \ddot{y}_d + v - k_2 \lceil s \rfloor^{\frac{1}{2}}, \tag{19b}$$

$$u_{eq} = -x_1 + \varepsilon \hat{x}_2 (1 - x_1^2) + \hat{x}_3 + \hat{k}_2 \lceil \hat{e}_1 \rfloor^{\frac{1}{3}}, \tag{19c}$$

$$\dot{v} = -k_3 \lceil s \rfloor^0, \tag{19d}$$

for some positive constants k_i, $i = \overline{1,3}$. The following result is provided.

Theorem 5. *Let the observer (6) and the controller (19) be applied to system (1) and Assumption 1 be satisfied. Let the observer parameters be chosen as in Theorem 2. Then, for some k_i, $i = \overline{1,3}$, the tracking error $e = 0$ is Uniformly Finite-Time Stable, for all $(\dot{f} + \dot{w}) \in \mathcal{L}_\xi$.*

Proof: Let us substitute (19) into the tracking error dynamics (10), *i.e.*

$$\dot{e}_1 = e_2, \tag{20a}$$

$$\dot{e}_2 = v - k_2 \lceil s \rfloor^{\frac{1}{2}} + \hat{e}_3, \tag{20b}$$

$$\dot{v} = -k_3 \lceil s \rfloor^0. \tag{20c}$$

Thus, since $\bar{e}_2 = e_2 - \hat{e}_2$, the closed-loop dynamics is given as

$$\Pi_{cst} : \begin{cases} \dot{e}_1 = \bar{e}_2 + \hat{e}_2, \\ \dot{\bar{e}}_2 = v - k_2 \lceil s \rfloor^{\frac{1}{2}}, \\ \dot{v} = -k_3 \lceil s \rfloor^0, \end{cases} \tag{21a}$$

$$\Pi_2 : \begin{cases} \dot{\hat{e}}_1 = \hat{e}_2 - \hat{k}_1 \lceil \hat{e}_1 \rfloor^{\frac{2}{3}}, \\ \dot{\hat{e}}_2 = \hat{e}_3 - \hat{k}_2 \lceil \hat{e}_1 \rfloor^{\frac{1}{3}}, \\ \dot{\hat{e}}_3 = -\hat{k}_3 \lceil \hat{e}_1 \rfloor^0 + \dot{f} + \dot{w}. \end{cases} \tag{21b}$$

Once again, system (21) can be viewed as a cascade system where Π_2 is the input of Π_{cst}. In this vein, this proof follows the same spirit as the proof of Theorem 4.

It has been already proven that system Π_2 converges to zero in a finite time, and moreover, that for all $t \geq 0$ and all $|\dot{f} + \dot{w}|_\infty \leq \xi$, $||\hat{e}(t, \hat{e}_0, \dot{f} + \dot{w})|| \leq \delta_{\hat{e}}$, for some $\delta_{\hat{e}} \geq 0$.

Then, for system Π_{cst}, let us define the following set-valued map

$$\tilde{F}(\bar{e}, v, \hat{e}_2) = \begin{pmatrix} F(\bar{e}, v, \hat{e}_2) \\ 0 \end{pmatrix} = \begin{pmatrix} \bar{e}_2 + \hat{e}_2 \\ v - k_2 \lceil s \rfloor^{\frac{1}{2}} \\ -k_3 \lceil s \rfloor^0 \\ 0 \end{pmatrix},$$

with $\bar{e} := (e_1, \bar{e}_2)^T \in \mathbb{R}^2$. This discontinuous function is homogeneous of degree $q = -1$ and weights $r = (3, 2, 1)$ and $\tilde{r} = 2$. In [19], it has been proven that, for $\hat{e}_2 = 0$, the quadratic form $V = \zeta^T P \zeta$, with $\zeta^T = (\ \lceil e_1 \rfloor^{\frac{2}{3}} \quad s \quad \lceil v \rfloor^2\ )$ and some $0 < P^T = P \in \mathbb{R}^{3\times 3}$, is a Lyapunov function for Π_{cst} such that, for some k_i, $i = \overline{1,3}$, $\dot{V} \leq -\kappa V^{3/4}$, with some positive κ. Therefore, $(\bar{e}, v) = 0$ is *UFTS*. Moreover, it is given that

$$||F(\bar{e}, v, \hat{e}_2) - F(\bar{e}, v, 0)|| = ||\hat{e}_2|| \leq \sigma(||\hat{e}_2||),\ \forall e_1, \bar{e}_2, v \in \mathbb{R},$$

$$\sigma(s) = \begin{cases} c s^{\rho_{\min}}, & if\ s \leq 1, \\ c s^{\rho_{\max}}, & if\ s > 1, \end{cases}$$

for $c \geq 1$ and $\rho_{\max} = \rho_{\min} = 1$. Hence, all the conditions of Theorem 1 hold, and due to $\tilde{r}_{\min} = 2 > 0$, system Π_{cst} is *FT-ISS* with respect to the bounded input $\hat{e}_2$, *i.e.*

$$\left\| \begin{matrix} \bar{e}(t, \bar{e}_0, v, \hat{e}_2) \\ v(t, e, v_0, \hat{e}_2) \end{matrix} \right\| \leq \beta_{cst} \left(\left\| \begin{matrix} \bar{e}_0 \\ v_0 \end{matrix} \right\|, t \right) + \gamma_{\hat{e}3}(||\hat{e}_2||_\infty), \tag{22}$$

for all $t \geq 0$ and some $\beta_{cst} \in \mathcal{KL}_T$ and $\gamma_{\hat{e}3} \in \mathcal{K}$. Additionally, since for system Π_2, $\hat{e} = 0$ is *UFTS*, (22) satisfies

$$\left\| \begin{matrix} \bar{e}(t, \bar{e}_0, v, \hat{e}_2) \\ v(t, e, v_0, \hat{e}_2) \end{matrix} \right\| \leq \beta_{cst} \left(\left\| \begin{matrix} \bar{e}_0 \\ v_0 \end{matrix} \right\|, t \right) + \gamma_{\hat{e}4}(||\hat{e}_2(0)||, t),$$

for all $t \geq 0$ and some $\beta_{cst}, \gamma_{\hat{e}4} \in \mathcal{KL}_T$. This implies $(\bar{e}, v) = 0$ is also *UFTS* for any $\hat{e}_2 \in \mathbb{R}$. Then, since $\hat{e}(t) = 0$ for some $t \geq \hat{T}$, it follows that $x_1(t) = y_d(t)$ and $x_2(t) = \dot{y}_d(t)$ for all $t \geq T_{cst}$, with some $T_{cst} > \hat{T}$. The proof is concluded. ■

It is worth mentioning that, unfortunately, there is not a constructive way to design the controller gains. However, one can try to use the same procedure as in Theorem 5, *i.e.* $k_1 > 0$ and $(k_2, k_3)^T = P^{-1}Y$.

E. Continuous Nonsingular Terminal Sliding-Mode Control Design

Let us consider the Continuous Nonsingular Terminal Sliding-Mode control (*Continuous*-NTSMC) [22], *i.e.*

$$s = e_1 + k_1 \lceil \bar{e}_2 \rfloor^{\frac{3}{2}}, \tag{23a}$$

$$u = -u_{eq} + \ddot{y}_d + v - k_2 \lceil s \rfloor^{\frac{1}{3}}, \tag{23b}$$

$$u_{eq} = -x_1 + \varepsilon \hat{x}_2 (1 - x_1^2) + \hat{x}_3 + \hat{k}_2 \lceil \hat{e}_1 \rfloor^{\frac{1}{3}}, \tag{23c}$$

$$\dot{v} = -k_3 \lceil s \rfloor^0, \tag{23d}$$

with some positive constants k_i, $i = \overline{1,3}$. The following result is established.

Theorem 6. *Let the observer (6) and the controller (23) be applied to system (1) and Assumption 1 be satisfied. Let the observer parameters be chosen as in Theorem 2. Then, for some k_i, $i = \overline{1,3}$, the tracking error $e = 0$ is Uniformly Finite-Time Stable, for all $(\dot{f} + \dot{w}) \in \mathcal{L}_\xi$.*

Proof: Let us replace control (23) into the tracking error dynamics (10), *i.e.*

$$\dot{e}_1 = e_2, \tag{24a}$$

$$\dot{e}_2 = v - k_2 \lceil s \rfloor^{\frac{1}{3}} + \hat{e}_3, \tag{24b}$$

$$\dot{v} = -k_3 \lceil s \rfloor^0. \tag{24c}$$

Note that $\bar{e}_2 = e_2 - \hat{e}_2$, then the closed-loop dynamics is described as follows

$$\Pi_{cnt} : \begin{cases} \dot{e}_1 = \bar{e}_2 + \hat{e}_2, \\ \dot{\bar{e}}_2 = v - k_2 \lceil s \rfloor^{\frac{1}{3}}, \\ \dot{v} = -k_3 \lceil s \rfloor^0, \end{cases} \tag{25a}$$

$$\Pi_2 : \begin{cases} \dot{\hat{e}}_1 = \hat{e}_2 - \hat{k}_1 \lceil \hat{e}_1 \rfloor^{\frac{2}{3}}, \\ \dot{\hat{e}}_2 = \hat{e}_3 - \hat{k}_2 \lceil \hat{e}_1 \rfloor^{\frac{1}{3}}, \\ \dot{\hat{e}}_3 = -\hat{k}_3 \lceil \hat{e}_1 \rfloor^0 + \dot{f} + \dot{w}. \end{cases} \tag{25b}$$

System Π_2 converges to zero in a finite time and for all $t \geq 0$ and all $|\dot{f} + \dot{w}|_\infty \leq \xi$, $||\hat{e}(t, \hat{e}_0, \dot{f} + \dot{w})|| \leq \delta_{\hat{e}}$, for some $\delta_{\hat{e}} \geq 0$. Then, for system Π_{cnt}, define the following set-valued map

$$\tilde{F}(\bar{e}, v, \hat{e}_2) = \begin{pmatrix} F(\bar{e}, v, \hat{e}_2) \\ 0 \end{pmatrix} = \begin{pmatrix} \bar{e}_2 + \hat{e}_2 \\ v - k_2 \lceil s \rfloor^{\frac{1}{3}} \\ -k_3 \lceil s \rfloor^0 \\ 0 \end{pmatrix}.$$

It is easy to show that this discontinuous function is also homogeneous of degree $q = -1$ and weights $r = (3, 2, 1)$ and $\tilde{r} = 2$. In [22], it is shown that, for $\hat{e}_2 = 0$, there exist coefficients $\beta > 0$ and $\gamma > 0$ such that the function

$$V(e, v) = \beta |e_1|^{\frac{5}{3}} + e_1 \bar{e}_2 + \frac{2}{5} k_1 |\bar{e}_2|^{\frac{5}{2}} - \frac{1}{k_1^3} \bar{e}_2 v^3 + \gamma |v|^5,$$

is a Lyapunov function for Π_{cnt} and for some k_i, $i = \overline{1,3}$, $\dot{V} \leq -\eta V^{4/5}$, with some positive η. Thus, this implies that $(\bar{e}, v) = 0$ is *UFTS*. The rest the proof follows the same steps as in the proof of Theorem 4 or 5, showing that system Π_{cnt} is also *FT-ISS* with respect to the bounded input $\hat{e}_2$.

Therefore, one concludes that $\bar{e} = 0$ is *UFTS* for some k_i, $i = \overline{1,3}$; and since $\hat{e}(t) = 0$ for some $t \geq \hat{T}$, hence, $x_1(t) = y_d(t)$ and $x_2(t) = \dot{y}_d(t)$ for all $t \geq T_{cnt}$, with some $T_{cnt} > \hat{T}$. ■

A possible selection for the gains k_i, $i = \overline{1,3}$, is given as follows [22]:

Table I
Continuous-NTSMC'S GAINS SELECTION

Set	**1**	**2**	**3**	**4**
k_1	$20\zeta^{-\frac{1}{2}}$	$28.7\zeta^{-\frac{1}{2}}$	$7.7\zeta^{-\frac{1}{2}}$	$\zeta^{-\frac{1}{2}}$
k_2	$4.4\zeta^{\frac{2}{3}}$	$4.5\zeta^{\frac{2}{3}}$	$7.5\zeta^{\frac{2}{3}}$	$16\zeta^{\frac{2}{3}}$
k_3	2.5ζ	2ζ	2ζ	7ζ
ζ	>0	>0	>0	>0

F. Continuous Twisting Control

Consider the Continuous Twisting control (*Continuous*-TC) [21], *i.e.*

$$u = -u_{eq} + \ddot{y}_d + v - k_1 \lceil e_1 \rfloor^{\frac{1}{3}} - k_2 \lceil \bar{e}_2 \rfloor^{\frac{1}{2}}, \tag{26a}$$

$$u_{eq} = -x_1 + \varepsilon \hat{x}_2 (1 - x_1^2) + \hat{x}_3 + \hat{k}_2 \lceil \hat{e}_1 \rfloor^{\frac{1}{3}}, \tag{26b}$$

$$\dot{v} = -k_3 \lceil e_1 \rfloor^0 - k_4 \lceil \bar{e}_2 \rfloor^0, \tag{26c}$$

with some positive constants k_j, $j = \overline{1,4}$. The following result is stated.

Theorem 7. *Let the observer (6) and the controller (26) be applied to system (1) and Assumption 1 be satisfied. Let the observer parameters be chosen as in Theorem 2. Then, for some k_i, $i = \overline{1,3}$, the tracking error $e = 0$ is Uniformly Finite-Time Stable, for all $(\dot{f} + \dot{w}) \in \mathcal{L}_\xi$.*

Proof: Substitute control (26) in the tracking error dynamics (10), *i.e.*

$$\dot{e}_1 = e_2, \tag{27a}$$

$$\dot{e}_2 = v - k_1 \lceil e_1 \rfloor^{\frac{1}{3}} - k_2 \lceil \bar{e}_2 \rfloor^{\frac{1}{2}} + \hat{e}_3, \tag{27b}$$

$$\dot{v} = -k_3 \lceil e_1 \rfloor^0 - k_4 \lceil \bar{e}_2 \rfloor^0. \tag{27c}$$

Recalling that $\bar{e}_2 = e_2 - \hat{e}_2$, the closed-loop dynamics can be written as follows

$$\Pi_{ct} : \begin{cases} \dot{e}_1 = \bar{e}_2 + \hat{e}_2, \\ \dot{\bar{e}}_2 = v - k_1 \lceil e_1 \rfloor^{\frac{1}{3}} - k_2 \lceil \bar{e}_2 \rfloor^{\frac{1}{2}}, \\ \dot{v} = -k_3 \lceil e_1 \rfloor^0 - k_4 \lceil \bar{e}_2 \rfloor^0, \end{cases} \tag{28a}$$

$$\Pi_2 : \begin{cases} \dot{\hat{e}}_1 = \hat{e}_2 - \hat{k}_1 \lceil \hat{e}_1 \rfloor^{\frac{2}{3}}, \\ \dot{\hat{e}}_2 = \hat{e}_3 - \hat{k}_2 \lceil \hat{e}_1 \rfloor^{\frac{1}{3}}, \\ \dot{\hat{e}}_3 = -\hat{k}_3 \lceil \hat{e}_1 \rfloor^0 + \dot{f} + \dot{w}. \end{cases} \tag{28b}$$

Then, according to Theorem 2, system Π_2 converges to zero in a finite time and for all $t \geq 0$ and all $|\dot{f} + \dot{w}|_\infty \leq \xi$, $||\hat{e}(t, \hat{e}_0, \dot{f} + \dot{w})|| \leq \delta_{\hat{e}}$, for some $\delta_{\hat{e}} \geq 0$. On the other hand, for system Π_{ct}, define the following set-valued map

$$\tilde{F}(\bar{e}, v, \hat{e}_2) = \begin{pmatrix} F(\bar{e}, v, \hat{e}_2) \\ 0 \end{pmatrix} = \begin{pmatrix} \bar{e}_2 + \hat{e}_2 \\ v - k_1 \lceil e_1 \rfloor^{\frac{1}{3}} - k_2 \lceil \bar{e}_2 \rfloor^{\frac{1}{2}} \\ -k_3 \lceil e_1 \rfloor^0 - k_4 \lceil \bar{e}_2 \rfloor^0 \\ 0 \end{pmatrix}.$$

This discontinuous vector field is homogeneous of degree $q = -1$ and weights $r = (3, 2, 1)$ and $\tilde{r} = 2$. In [21], it has been shown that, for $\hat{e}_2 = 0$, there exist coefficients β_j, $j = \overline{1,4}$, such that the function

$$V(\bar{e}, v) = \beta_1 |e_1|^{\frac{5}{3}} + \beta_2 e_1 \bar{e}_2 + \beta_3 |\bar{e}_2|^{\frac{5}{2}} + \beta_4 e_1 \lceil v \rfloor^2 - \beta_5 \bar{e}_2 v^3 + \beta_6 |v|^5,$$

is a Lyapunov function for system Π_{ct} and for some k_j, $j = \overline{1,4}$, $\dot{V} \leq -\gamma V^{4/5}$, with some positive γ. This implies that $(\bar{e}, v) = 0$ is *UFTS*. Then, note that

$$||F(\bar{e}, v, \hat{e}_2) - F(\bar{e}, v, 0)|| = ||\hat{e}_2|| \leq \sigma(||\hat{e}_2||), \ \forall e_1, \bar{e}_2, v \in \mathbb{R},$$

$$\sigma(s) = \begin{cases} c s^{\rho_{\min}}, & if \ s \leq 1, \\ c s^{\rho_{\max}}, & if \ s > 1, \end{cases}$$

for $c \geq 1$ and $\rho_{\max} = \rho_{\min} = 1$. Hence, following the same steps as in the proof of Theorem 4 or 5, one can show that system Π_{ct} is also *FT-ISS* with respect to the bounded input $\hat{e}_2$.

Therefore, one concludes that $\bar{e} = 0$ is *UFTS* for some k_j, $j = \overline{1,4}$. Since $\hat{e}(t) = 0$ for some $t \geq \hat{T}$, it follows that $x_1(t) = y_d(t)$ and $x_2(t) = \dot{y}_d(t)$ for all $t \geq T_{ct}$, with some $T_{ct} > \hat{T}$. The proof is concluded. ■

A possible choice for the gains k_j, $j = \overline{1,4}$, is given as follows [21]:

Table II
Continuous-TC'S GAINS SELECTION

Set	**1**	**2**	**3**	**4**
k_1	$25\zeta^{\frac{2}{3}}$	$19\zeta^{\frac{2}{3}}$	$13\zeta^{\frac{2}{3}}$	$7\zeta^{\frac{2}{3}}$
k_2	$15\zeta^{\frac{1}{2}}$	$10\zeta^{\frac{1}{2}}$	$7.5\zeta^{\frac{1}{2}}$	$5\zeta^{\frac{1}{2}}$
k_3	2.3ζ	2.3ζ	2.3ζ	2.3ζ
k_4	1.1ζ	1.1ζ	1.1ζ	1.1ζ
ζ	> 0	> 0	> 0	> 0

Remark 5. *It is worth mentioning that the proposed control strategy together with the five* Continuous SMCs *can be perfectly applied to any system described by a perturbed double integrator; for instance, DC servomotor [15], robotic manipulator [4], etc.*

Some theoretical comments about the proposed strategies:

1) All of the proposed control strategies are continuous and robust against the class of perturbations described by Assumption IV-A.
2) The Linear Control and the Super-Twisting Control approaches provide only *uniform exponential stability.*
3) The *Continuous*-STSMC, the *Continuous*-NTSMC and the *Continuous*-TC provide *uniform finite-time stability.* This represents the main theoretical difference between these three controllers and the two previous ones. Evidently, the finite-time stability is a stronger property than the exponential one, theoretically speaking.
4) The Linear Control has only two design gains and it is the simplest approach to implement which are the main advantages of this approach.
5) The Super-Twisting Control, the *Continuous*-STSMC and the *Continuous*-NTSMC have three design gains and they are more complex to implement due to the nonlinearities which can be seen as drawbacks with respect to the Linear Control.
6) The *Continuous*-TC has four design gains and the implementation complexity is similar to the other nonlinear controllers. In this sense, the *Continuous*-TC is the most complex to implement and design with respect to the other approaches.
7) The main advantage of the *Continuous*-STSMC, the *Continuous*-NTSMC and the *Continuous*-TC is the finite-time stability they provide for the same class of perturbations.
8) It is clear that there exist a trade-off between implementation and designing complexity, and the stability performance.

V. RESULTS AND DISCUSSIONS

A. Simulation Results

To demonstrate the performance of the *Continuous*-SMCs proposed in Section IV, numerical simulation studies are performed in this section. Model parameter $\varepsilon = 0.1$ is selected. Band-limited white noise is added in the output y to make the simulation realistic. $w(t) = \sin(3t) + 1$ is selected as the bounded Lipschitz disturbance in Eq. (1). The objective of the controllers is to track a sinusoidal reference $y_d(t) = \sin(2\pi t)$. The used parameters for the HOSM-O and the *Continuous*-SMCs are shown in Table III. As a comparison tool, an extended high-gain (EHG) observer based output-feedback control strategy [34] has been selected. The parameters of EHG controller are selected according to the guidelines given in [34] and avoided here for the purpose of brevity.

Table III
PARAMETERS OF THE CONTROL STRATEGIES

Parameter	**HOSM-O**	**Linear**	**Super Twisting**
$\hat{k}_1$ / k_1	11.0521	1	1
$\hat{k}_2$ / k_2	10.6066	3.6742	3.6742
$\hat{k}_3$ / k_3	55	–	6.6000
ξ / ζ	50	–	6

Parameter	**STSMC**	**NTSMC**	**TC**
k_1	1	3.1435	23.1135
k_2	3.6742	24.7645	12.2474
k_3	6.6000	12	13.8000
k_4	–	–	6.6000
ζ	6	6	6

The first step in applying the *Continuous*-SMCs is to estimate the states x_1 and x_2 as well as some perturbations from the noise corrupted measurement y. In the simulation, measurement noise has been added. The state estimation errors can be found

in Fig. 1. The Fig. 1 shows that the HOSM-O successfully estimated the states in a finite-time. Using the estimated states, the *Continuous*-SMCs (9), (13), (19), (23) and (26) are applied. EHG based output-feedback is also applied as a comparison tool. The tracking performance of the controllers are given in Fig. 2. The tracking error for different controllers is shown in Fig. 3. From Fig. 2 and 3, it can be seen that the performances of the various *Continuous*-SMCs are more or less the same. Except the compensation based linear control (9), the other *Continuous*-SMCs converged to the desired trajectory in a very short-time. However, the same cannot be said about EHG. It s clear that the EHG has very high peak amplitude for the states x_2. This impacts the settling time for x_1. Moreover, the steady state error for EHG is significantly higher than the *Continuous*-SMCs. As such this method has not been included in the further calculation for the sake of readability. This demonstrates the effectiveness of the applied *Continuous*-SMC control strategies for the Van der Pol oscillator. The control signals for all the SMC controllers are given in Fig. 4. The Fig. 4 shows that some SMC controllers require high amplitude in the transient period while others do not need it. High amplitude control signal may be problematic for some applications. In that case, saturation of the control signal can be done to prevent the damage of the plant being controlled.

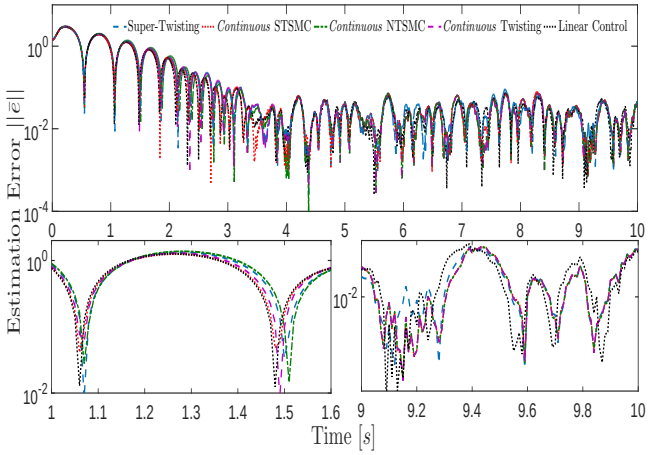

Figure 1. State estimation errors for each SMC control strategy. Zoomed versions are given in the bottom row.

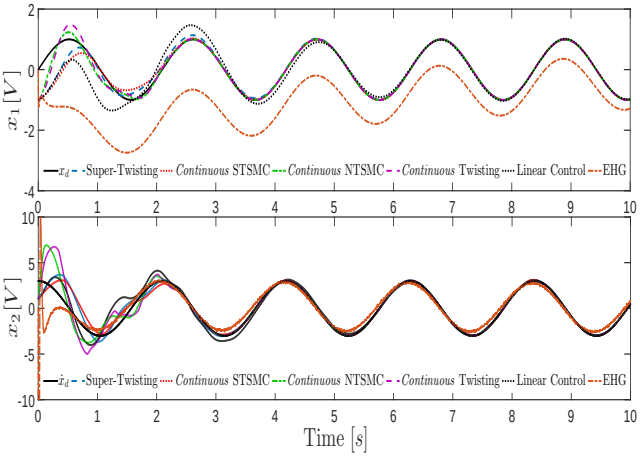

Figure 2. Comparative tracking performance for each control strategy.

B. Experimental Results

To validate the theoretical results presented in Section IV, an experimental study is considered in this section. For this purpose, model (1) has been constructed with parameter $\varepsilon \approx 0.1$. The electronic circuit diagram can be seen in Fig. 5.

The circuit parameters are: $R_i = 1M\Omega, i = \overline{1,6}$, $R_7 = 130\Omega$, $R_8 = 1.2K\Omega$, $R_9 = 100\Omega$, $R_{10} = 1.5K\Omega$, $C_1 = C_2 = 1\mu F$, LM741 is a general purpose operational amplifier and AD633 is a 4-quadrant multiplier operational amplifier. A dSPACE 1104 board was used as a rapid prototyping solution. The experimental setup was realized at Coventry University, United Kingdom. All the proposed controllers were implemented using Simulink. The solver was the Euler's method and the sampling frequency was 4KHz. The used parameters for the HOSM-O and the *Continuous*-SMCs for the experimental realization are shown in Table IV.

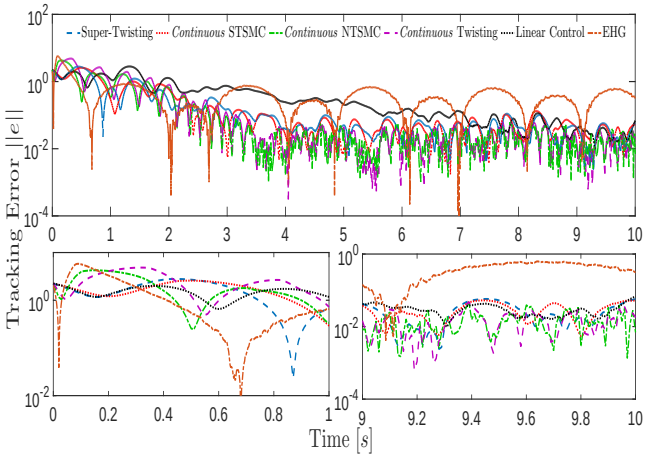

Figure 3. Tracking error performance for each control strategy. Zoomed versions are given in the bottom row.

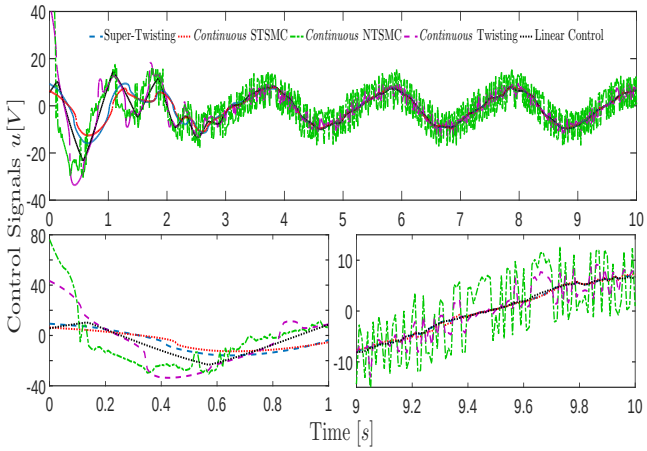

Figure 4. Control signals for each SMC control strategy. Zoomed versions are given in the bottom row.

Table IV
PARAMETERS OF THE CONTROL STRATEGIES

Parameter	HOSM-O	Linear	Super Twisting
$\hat{k}_1$ / k_1	6.86	1	1
$\hat{k}_2$ / k_2	5.1962	3.6742	3.6742
$\hat{k}_3$ / k_3	13.2	–	6.6000
ξ / ζ	12	–	6

Parameter	STSMC	NTSMC	TC
k_1	1	0.4082	23.1135
k_2	3.6742	52.8308	12.2474
k_3	6.6000	42	13.8000
k_4	–	–	6.6000
ζ	6	6	6

Remark 6. The existing literature on the SMC discretization techniques [35], [36] suggested the use of implicit Euler technique which is computationally complex for real-time implementation. Explicit Euler technique is computationally simple and easy to implement in real-time. In [36], it has been shown that for sufficiently small sampling frequency, the explicit Euler technique converges to the vicinity of the origin, which is acceptable for practical application. It is to be noted here that due to the discretization of continuous controllers, only practical finite-time stability instead of finite-time stability can be achieved in practice.

The objective here is to track a reference signal $y_d = x_d = \sin(3t)$. The experimental results for sinusoidal reference tracking are given in Fig. 6. This figure shows that all the controllers successfully tracked the time varying reference signal. The performance of the controllers are almost identical in the steady-state. In the transient regime, *Continuous*-NTSMC and compensation based linear controller behaved differently than the others. For example, the settling time of *Continuous*-NTSMC

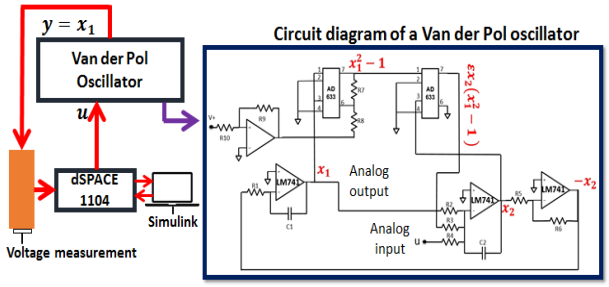

Figure 5. Experimental setup

and linear control are significantly higher than the others. Moreover, *Continuous*-NTSMC has large overshoot than the others. One explanation for this particular behavior of the *Continuous*-NTSM is due to the control magnitude.

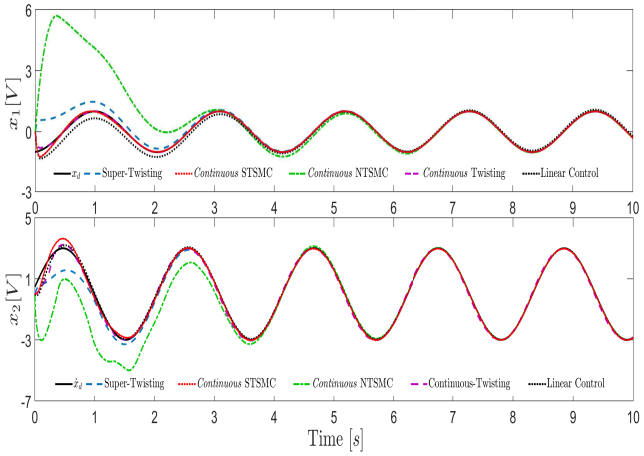

Figure 6. Experimental results for sinusoidal reference tracking.

The control signals for sinusoidal reference tracking can be found in Fig. 7. This figure shows that the amplitude of *Continuous*-NTSMC is higher than the others. This causes the large overshoot in the transient period. If the gains of *Continuous*-NTSMC are reduced, then the maximum overshoot value decreases but increases the settling time. As a result some trade-offs have to be made for the selection of control gains of *Continuous*-NTSMC. The control profile of *Continuous*-Twisting is similar to that of *Continuous*-NTSMC just the magnitude is smaller. If the gains of *Continuous*-Twisting are reduced following the guidelines provided in Table II, the control profile become smoother but increases the settling time. Thus, some trade-offs have to be made for the selection of control gains of *Continuous*-Twisting.

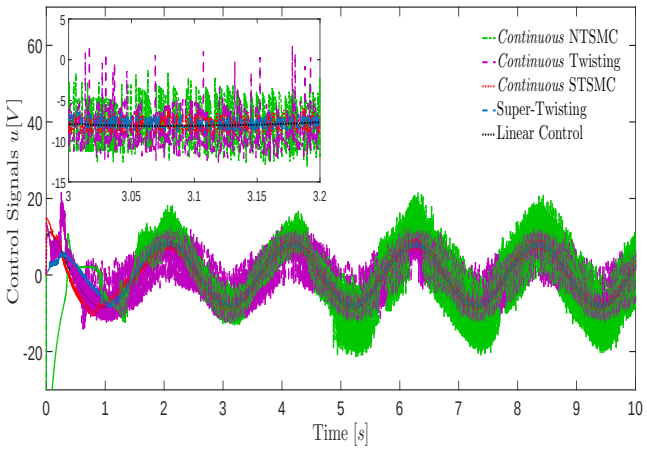

Figure 7. Control signals for experimental sinusoidal reference tracking

Although *Continuous*-SMCs are developed for the robust output tracking Fig. 7 shows that some control signals are not very smooth. In an experimental settings, the controller needs to compensate the nonlinearities and nonidealities of the practical device which are not included in the mathematical model. Moreover, practical devices that implement the controller work in discrete time time and digital domain. So, analog-to-digital and digital-to-analog conversions are required. This also introduces conversion error and the error depends on the device being used for control implementation. All these factors contribute to the not so smooth control profile.

In the simulation, it is observed that the convergence time of the compensation based linear control is significantly higher than the other controllers. Same thing can be observed in the experiment also. Except *Continuous*-NTSMC, the other controllers converged at a rate much faster than the compensation based linear controller. Moreover, the tracking error magnitude is also relative high for the linear controller. This justifies the use of robust control over compensation based linear control.

To formally compare the controllers in a constructive manner, time domain performance criteria are very useful. They are widely used in the standard literature for comparison purpose. In this work, three criteria have been selected namely - settling time, Maximum Steady State Error (MSSE), and the energy of the control signal. The first two criteria can be found from the Root Mean Square (RMS) plot of the tracking error signal while the third can be obtained from RMS plot of the control signal. The following definition of RMS values will be used.

$$e_{1\text{RMS}} = \sqrt{\frac{1}{\Delta T}\int_{t-\Delta t}^{t} (\hat{x}_1(\tau) - x_d(\tau))^2 d\tau}, \tag{29}$$

$$u_{\text{RMS}} = \sqrt{\frac{1}{\Delta T}\int_{t-\Delta t}^{t} u^2(\tau) d\tau}, \tag{30}$$

where ΔT is the interval over which the RMS value is computed. A 30 samples window is selected to calculate the RMS value. The RMS profile of the tracking error and control signal can be seen in Fig. 8.

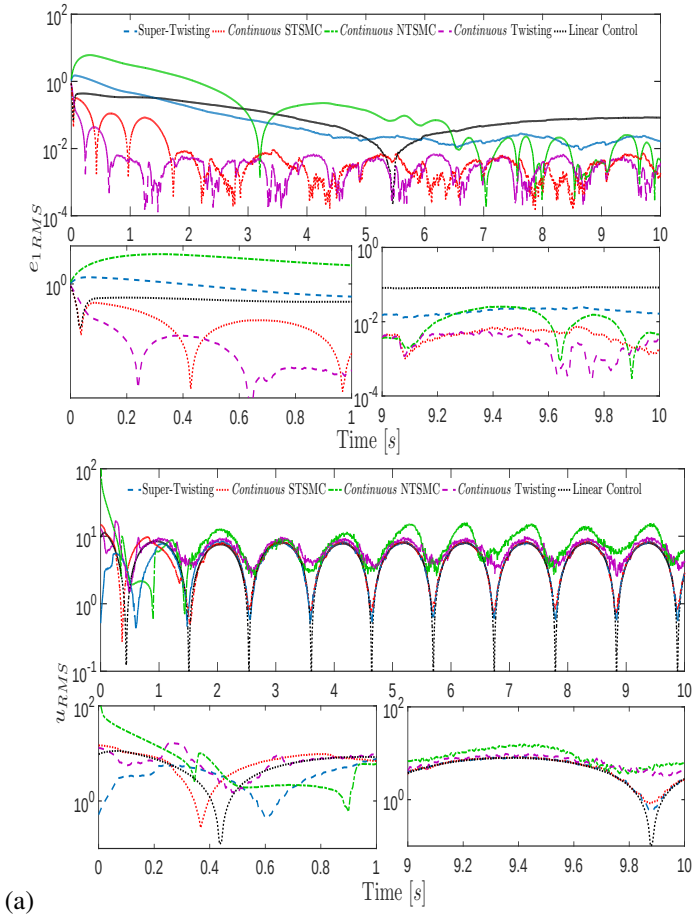

Figure 8. R.M.S. values: a) tracking error for various SMC controllers; b) control signals for sinusoidal reference tracking.

Time domain performance criteria of the controllers are tabulated in Table V. From Table V, it can be seen that there is no absolute winner. The *Continuous*-Twisting controller has very good settling time and MSSE performance but the maximum control energy being used in the steady state is sufficiently high. The *Continuous*-STSMC and Super Twisting controller both are using same control energy but *Continuous*-STSMC outperform Super Twisting in other criteria. Although MSSE performance of *Continuous*-NTSMC is better than linear control, this one is using double energy than the linear one. Based on Table V, from practical point of view it can be said that *Continuous*-STSMC is the best performing one among the others. It has slight higher settling time than *Continuous*-Twisting but the MSSE and control energy point of view the performance is very close to the best performing controllers in each category.

Table V
TIME DOMAIN PERFORMANCE SUMMARY OF VARIOUS *Continuous*-SMCS

Parameter	**Linear**	**Super Twisting**	
Settling Time	3.3	2.35	
MSSE	0.132	0.025	
max $\{u_{\text{RMS}}\}$	8	8.4	
Parameter	**STSMC**	**NTSMC**	**TC**
Settling Time	0.3085	5.07	0.08
MSSE	0.008	0.022	0.007
max $\{u_{\text{RMS}}\}$	8.4	16.38	9.5

Finally, based on the experimental results, it can be said that experimental results validate the theoretical developments of Sec. IV.

VI. CONCLUSION

This paper studies the problem of tracking control design for the Van der Pol oscillator. Output feedback based robust tracking control strategies are proposed in this work for that purpose. First, a HOSM-O is used to estimate the oscillator states from the measurable output and to identify some type of disturbances. Then, five different *Continuous*-SMCs are provided to robustly track a desired time-varying trajectory, exponentially or in a finite time, for the Van der Pol oscillator despite the presence of external disturbances. The closed-loop stability for each *Continuous*-SMC is given based on ISS properties. Finally, experimental validations are also provided to show the feasibility of the proposed controllers in real-time.

REFERENCES

[1] H. Li and Y. Cai, "On sftsm control with fixed-time convergence," *IET Control Theory & Applications*, vol. 11, no. 6, pp. 766–773, 2017.

[2] I. Salgado, M. Mera, and I. Chairez, "Suboptimal adaptive control of dynamic systems with state constraints based on barrier lyapunov functions," *IET Control Theory & Applications*, 2018.

[3] C. U. Solis, J. B. Clempner, and A. S. Poznyak, "Fast terminal sliding-mode control with an integral filter applied to a van der pol oscillator," *IEEE Trans Ind Electron*, vol. 64, no. 7, pp. 5622–5628, July 2017.

[4] I. Salgado, I. Chairez, O. Camacho, and C. Yañez, "Super-twisting sliding mode differentiation for improving pd controllers performance of second order systems," *ISA Trans*, vol. 53, no. 4, pp. 1096–1106, 2014.

[5] B. Kaplan, I. Gabay, G. Sarafian, and D. Sarafian, "Biological applications of the "filtered" van der pol oscillator," *J Franklin Inst*, vol. 345, no. 3, pp. 226–232, 2008.

[6] B. B. Johnson, M. Sinha, N. G. Ainsworth, F. Dörfler, and S. V. Dhople, "Synthesizing virtual oscillators to control islanded inverters," *IEEE Trans Power Electron*, vol. 31, no. 8, pp. 6002–6015, 2016.

[7] H. Ahmed, R. Ushirobira, D. Efimov, D. Tran, M. Sow, P. Ciret, and J.-C. Massabuau, "Monitoring biological rhythms through the dynamic model identification of an oyster population," *IEEE Transactions on Systems, Man, and Cybernetics: Systems*, vol. 47, no. 6, pp. 939–949, 2017.

[8] Y. Orlov, L. T. Aguilar, L. Acho, and A. Ortiz, "Asymptotic harmonic generator and its application to finite time orbital stabilization of a friction pendulum with experimental verification," *Int J Control*, vol. 81, no. 2, pp. 227–234, 2008.

[9] J.-X. Xu, Y.-J. Pan, and T.-H. Lee, "Sliding mode control with closed-loop filtering architecture for a class of nonlinear systems," *IEEE Trans Circuits Syst II Express Briefs*, vol. 51, no. 4, pp. 168–173, 2004.

[10] A. J. Calise, N. Hovakimyan, and M. Idan, "Adaptive output feedback control of nonlinear systems using neural networks," *Automatica*, vol. 37, no. 8, pp. 1201–1211, 2001.

[11] N. Hovakimyan, F. Nardi, A. Calise, and N. Kim, "Adaptive output feedback control of uncertain nonlinear systems using single-hidden-layer neural networks," *IEEE Trans Neural Networks*, vol. 13, no. 6, pp. 1420–1431, 2002.

[12] W. He, H. Huang, and S. S. Ge, "Adaptive neural network control of a robotic manipulator with time-varying output constraints," *IEEE transactions on cybernetics*, vol. 47, no. 10, pp. 3136–3147, 2017.

[13] H. Zhang, X.-Y. Wang, and X.-H. Lin, "Topology identification and module–phase synchronization of neural network with time delay," *IEEE Transactions on Systems, Man, and Cybernetics: Systems*, vol. 47, no. 6, pp. 885–892, 2017.

[14] J. J. Rath, M. Defoort, H. R. Karimi, and K. C. Veluvolu, "Output feedback active suspension control with higher order terminal sliding mode," *IEEE Trans Ind Electron*, vol. 64, no. 2, pp. 1392–1403, Feb 2017.

[15] S. K. Kommuri, J. J. J. Rath, and K. C. Veluvolu, "Sliding mode based observer-controller structure for fault-resilient control in dc servomotors," *IEEE Trans Ind Electron*, vol. 65, no. 1, pp. 918 – 929, 2018.

[16] M. Basin, P. Yu, and Y. Shtessel, "Hypersonic missile adaptive sliding mode control using finite- and fixed-time observers," *IEEE Trans Ind Electron*, vol. 65, no. 1, pp. 930–941, 2018.

[17] A. Chalanga, S. Kamal, L. M. Fridman, B. Bandyopadhyay, and J. A. Moreno, "Implementation of super-twisting control: Super-twisting and higher order sliding-mode observer-based approaches," *IEEE Trans Ind Electron*, vol. 63, no. 6, pp. 3677–3685, 2016.

[18] N. Xavier, B. Bandyopadhyay, and R. Schmid, "Robust non-overshooting tracking using continuous control for linear multivariable systems," *IET Control Theory & Applications*, vol. 12, no. 7, pp. 1006 – 1011, 2018.

[19] L. Fridman, J. A. Moreno, B. Bandyopadhyay, S. Kamal, and A. Chalanga, "Continuous nested algorithms: The fifth generation of sliding mode controllers," in *Recent Advances in Sliding Modes: From Control to Intelligent Mechatronics*, X. Yu and M. O. Efe, Eds. Springer International Publishing, 2016, ch. 2, pp. 5–35.

[20] A. Levant, "Higher-order sliding modes, differentiation and output-feedback control," *Int J Control*, vol. 76, no. 9-10, pp. 924–941, 2003.

[21] V. Torres-Gonzalez, T. Sanchez, L. M. Fridman, and J. A. Moreno, "Design of continuous twisting algorithm," *Automatica*, vol. 80, pp. 119–126, 2017.

[22] S. Kamal, J. A. Moreno, A. Chalanga, B. Bandyopadhyay, and L. M. Fridman, "Continuous terminal sliding-mode controller," *Automatica*, vol. 69, pp. 308–314, 2016.

[23] J. Song, Y. Niu, and Y. Zou, "Finite-time stabilization via sliding mode control," *IEEE Transactions on Automatic Control*, vol. 62, no. 3, pp. 1478–1483, 2017.

[24] N. Vazquez, J. Vazquez, J. Vaquero, C. Hernandez, E. Vazquez, and R. Osorio, "Integrating two stages as a common-mode transformerless photovoltaic converter," *IEEE Trans Ind Electron*, vol. 64, no. 9, pp. 7498 – 7507, 2017.

[25] A. Levant, "Sliding order and sliding accuracy in sliding mode control," *Int J Control*, vol. 58, no. 6, pp. 1247–1263, 1993.

[26] ——, "Robust exact differentiation via sliding mode technique," *automatica*, vol. 34, no. 3, pp. 379–384, 1998.

[27] D. Efimov, A. Levant, A. Polyakov, and W. Perruquetti, "Supervisory acceleration of convergence for homogeneous systems," *Int J Control*, no. 0, pp. 1–11, 2017.

[28] A. Bacciotti and L. Rosier, *Liapunov functions and stability in control theory*, ser. Communications and Control Engineering. Berlin: Springer, 2001.

[29] V. Zubov, "On systems of ordinary differential equations with generalized homogenous right-hand sides." *Izvestia vuzov. Mathematica*, vol. 1, pp. 80–88, 1958.

[30] E. Bernuau, D. Efimov, W. Perruquetti, and A. Polyakov, "On homogeneity and its application in sliding mode control," *J Franklin Inst*, vol. 351, no. 4, pp. 1866–1901, 2014.

[31] S. Dashkovskiy, D. V. Efimov, and E. D. Sontag, "Input to state stability and allied system properties," *Autom Remote Control*, vol. 72, no. 8, pp. 1579–1614, 2011.

[32] E. Cruz-Zavala and J. A. Moreno, "Lyapunov functions for continuous and discontinuous differentiators," *IFAC-PapersOnLine*, vol. 49, no. 18, pp. 660–665, 2016.

[33] J. A. Moreno, "Lyapunov approach for analysis and design of second order sliding mode algorithms," *Sliding Modes after the first decade of the 21st Century*, vol. 412, pp. 113–149, 2011.

[34] H. H. Khalil, *High-Gain Observers in Nonlinear Feedback Control*. SIAM, 2017, vol. 31.

[35] V. Acary and B. Brogliato, "Implicit euler numerical scheme and chattering-free implementation of sliding mode systems," *Systems & Control Letters*, vol. 59, no. 5, pp. 284–293, 2010.

[36] D. Efimov, A. Polyakov, A. Levant, and W. Perruquetti, "Realization and discretization of asymptotically stable homogeneous systems," *IEEE Transactions on Automatic Control*, vol. 62, no. 11, pp. 5962–5969, 2017.